ASTROBIOLOGY
Volume 12, Number 8, 2012

DOI: 10.1089/ast.2011.0763

Using a Mini-Raman Spectrometer to Monitor the Adaptive Strategies of Extremophile Colonizers in Arid Deserts: Relationships Between Signal Strength, Adaptive Strategies, Solar Radiation, and Humidity

I. Miralles,[1] S.E. Jorge-Villar,[2] Y. Cantón,[3] and F. Domingo[1]

Abstract

The survival strategies of one cyanobacteria colony and three terricolous lichen species from the hot subdesert of Tabernas, Spain, were studied along with topographical attributes of the area to investigate whether the protective strategies adopted by these pioneer soil colonizers are related to the environmental stressors under which they survive. A handheld Raman spectrometer was used for biomolecular characterization, while the microclimatic and topographic parameters were estimated with a Geographic Information System (GIS). We found that the survival strategies adopted by those organisms are based on different combinations of protective biomolecules, each with diverse ecophysiological functions, such as UV-radiation screening, free-energy quenching, antioxidants, and the production of different types and amounts of calcium oxalates. Our results show that the cyanobacteria community and each lichen species preferentially colonized a particular microhabitat with specific moisture and incident solar radiation levels and exhibited different adaptive mechanisms. In recent years, a number of studies have provided consistent results that suggest a link between the strategies adopted by those extremophile organisms and the microclimatic environmental parameters. To date, however, far too little attention has been paid to results from Raman analyses on dry specimens. Therefore, the results of the present study, produced with the use of our miniaturized instrument, will be of interest to future studies in astrobiology, especially due to the likely use of Raman spectroscopy at the surface of Mars. Key Words: Hot desert—Raman spectroscopy—Topography—Terricolous lichens—Cyanobacteria—Planetary exploration. Astrobiology 12, 743–753.

1. Introduction

Lichens and cyanobacteria have the capacity to survive extreme environmental conditions because of their ability to develop a variety of protective strategies. Such strategies include both bio- and geoprotective mechanisms that allow these extremophiles to colonize a wide range of habitats (Edwards *et al.*, 2003a). In cold and hot deserts, extreme environments that are well distributed around Earth, temperature fluctuation, low humidity, and harmful solar radiation are all important ecosystem stressors (Cockell and Knowland, 1999; Dickensheets *et al.*, 2000). Lichens and cyanobacteria are well-known primo colonizers on rocks and soils and have developed a large number of protective strategies to withstand such hazardous conditions (Jorge-Villar *et al.*, 2005a).

Synthesis of biochemical metabolites, such as oxalates, carotenoids, chlorophyll, parietin, emodin, atranorin, gyrophoric acid, fumarprotocetraric acid, rhizocarpic acid, calycin, usnic acid, and so on, is a common strategy against some extreme conditions. Such biomolecules and pigments play important roles as antidesiccants and water-replacement molecules, UV-radiation screen compounds, antioxidants, DNA repair agents, or energy-quenching molecules (Nealson, 1997; Cockell and Knowland, 1999; Wynn-Williams and Edwards, 2000; Edwards, 2007).

In recent years, there has been an increasing interest in the detection of biochemical metabolites produced by lichens and cyanobacteria colonies in response to external stress as a vital part of understanding life processes under hostile conditions (Jorge-Villar and Edwards, 2010). Nevertheless, despite the critical role of protective pigments in lichen and cyanobacteria survival, little is known about their specific biological role, and in fact, the dynamics of those communities have rarely been studied. Furthermore, few studies

[1]Experimental Station of Arid Zones (CSIC), Almería, Spain.
[2]University of Burgos, Area de Geodinamica Interna, Facultad de Humanidades y Educacion, Burgos, Spain.
[3]University of Almería, Departamento de Edafologia y Quimica Agricola, Almería, Spain.

have attempted to discern whether environmental factors regulate pigment synthesis in such communities (Garcia-Pichel and Castenholz, 1991; Ehling-Schulz *et al.*, 1997; Sinha *et al.*, 2001; Dillon *et al.*, 2002; Singh *et al.*, 2011).

The study of survival strategies developed by extremophiles would provide significant assistance to the effort of understanding the distribution of life under severe environmental conditions. Knowing which chemicals could serve as signatures of terrestrial life in extreme habitats, such as hot or cold deserts or acidic or alkaline waters, would help in the design of improved instruments for the detection of life on other planetary surfaces.

Raman spectroscopy stands out among analytical techniques as the most suitable for identifying organic and inorganic compounds in these extreme conditions (Edwards *et al.*, 1999, 2003a, 2003b; Wang *et al.*, 2004). It provides molecular information and is able to characterize any mixture of organic and inorganic compounds, including polymorphous and isomorphous differentiation. No chemical or physical sample manipulation is necessary, and micro- as well as macrospecimens can be analyzed. Furthermore, it is a nondestructive technique, so that after analyses the sample can be completely recovered and reused. Development of small commercial handheld Raman spectrometers, with long-lasting batteries and optical fibers, makes it possible to conduct on-site field measurements. These characteristics have made Raman spectroscopy an important technique in astrobiology such that it is currently being considered by NASA and ESA for use in martian surface exploration (Jorge-Villar and Edwards, 2005).

Desert habitats are considered plausible analogues for possible extraterrestrial life. Studying and understanding the adaptive mechanisms of extremophiles in desert environments, and the subsequent recognition of biomarkers, will be of great help in the search for life on extraplanetary surfaces. This is of particular interest for the identification of possible signs of life on Mars, since at this point in its geological evolution there is little or no liquid water on its surface. To date, investigations of biomarkers and survival strategies adopted by extremophiles in which Raman spectroscopy has been used have focused primarily on cold deserts (Wynn-Williams and Edwards, 2000; Edwards *et al.*, 2003a, 2004a, 2004b, 2005; Jorge-Villar *et al.*, 2005b), and only a few studies have been carried out in hot deserts (Jorge-Villar *et al.*, 2005a; Jorge-Villar and Edwards, 2010). It would, therefore, be of great interest to compare the survival strategies of extremophiles in hot deserts with those in cold deserts. Since we do not know whether life exists, or existed, on Mars, nor do we know where or when life might have occurred, we can only speculate as to the environmental conditions under which life might have subsisted. Nevertheless, it is frequently assumed that, during the final period when life may have existed on Mars, conditions were likely to have been cold and dry. It would, therefore, be useful to employ Raman spectroscopy to study as many terrestrial habitats as possible to discern whether different survival strategies can be detected. Obviously, the biomolecular degradation could be different under hot or cold conditions, which would lead to different spectroscopic signatures. The identification of those spectral characteristics is of vital importance for the recognition of life's signals. These studies begin, on Earth, with the identification of different adaptive strategies in extreme environments and their comparison for a deeper understanding and interpretation of Raman spectra. The Tabernas Desert, located in southeast Spain, is a unique environment in Europe for its arid climate, geomorphological dynamics, biodiversity, and endemic species, and it is therefore an ideal scenario for this type of study. Vegetation is sparse or, in places, absent in this region's intensely dissected natural badlands landscape (Bryan and Yair, 1982), which is characterized by a dense drainage network and short steep slopes with narrow watersheds (Scheidegger *et al.*, 1968). Geomorphologically, badlands are like a miniature desert developed on nonconsolidated and relatively impermeable material that is exposed to rapid water erosion (Campbell, 1989). Both lithology and climate determine the geomorphological dynamics of this system, which form an extremely complex topography, and as a result, important microclimatic variations are noticeable within short distances (Cantón *et al.*, 2001). Significant differences in slope, aspect, insolation, and humidity typical of the badlands could induce primary colonizing species, such as lichens and cyanobacteria, to develop specific adaptive strategies in these extreme, dynamic, and active environments.

We present here, for the first time, a Raman spectroscopy study of four extremophile organisms from the Tabernas Desert (Spain): a cyanobacteria colony and three lichen species. Insolation and other topographical environmental parameters of this hostile habitat were analyzed within a Geographic Information System (GIS) in an attempt to relate the biostrategies developed by the four organisms with environmental parameters as well as with their field distribution. The combination of both analytical techniques would be valuable for obtaining complementary information about complex adaptation strategies to environmental factors implemented by different extremophile communities.

2. Methodology

2.1. Experimental area

The study area, the Tabernas Desert in southeastern Spain (Province of Almería), is one of the largest badlands in Europe with an area of 150 km^2. It is located in the Sorbas–Tabernas basin and surrounded by several Betic ranges: the Gador, Nevada, Filabres, and Alhamilla Mountains (Fig. 1). Specifically, the study site is a 12.65-hectare gully, located between 37°0′40″N, 2°26′29″W and 37°0′55″N, 2°26′10″W. The altitude ranges from 247.5 to 382.5 m. The landscape is characterized by its complex geomorphology with bare, eroded, and poorly developed soils (Epileptic Regosol) in steeper southwest-facing slopes (gradients up to 70°). In contrast, northeast-facing slopes with gradients less than 30° usually have more developed soils (Endoleptic Regosols) that are covered with biological crusts, including many species of terricolous lichens such as *Diploschistes diacapsis, Squamarina lentigera,* and *Lepraria crassissima* as well as cyanobacteria. At the pediments, on gentle slope gradients, soils are thicker (Haplic Calcisol) (Miralles-Mellado *et al.*, 2011) and covered by biological soil crusts in open areas with patches of annual plants (dominated by *Stipa capensis*) and scattered perennial plants (with predominance of *Helianthemun almeriense, Hammada articulata, Artemisia barrelieri, Salsola genistoides*).

The lithology is mainly a carbonated-gypsiferous Miocene mudstone, and the average mineralogical composition is

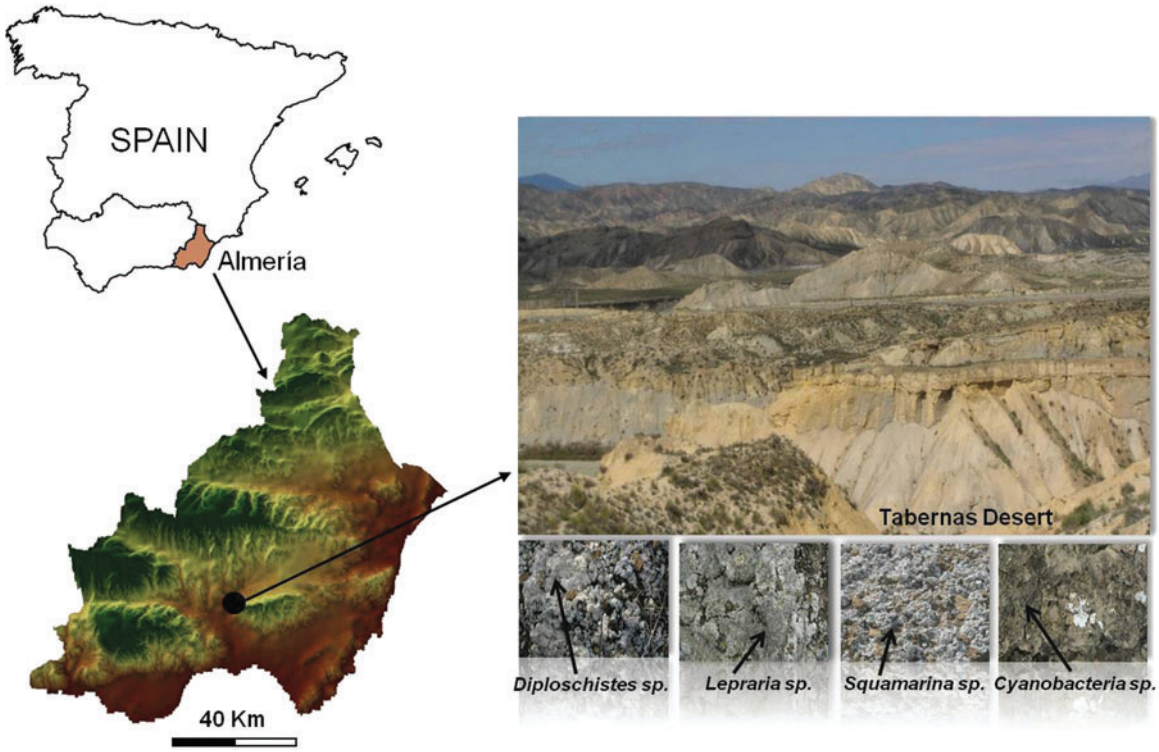

FIG. 1. Study area and specimens. Color images available online at www.liebertonline.com/ast

muscovite 35%, paragonite 10%, chlorite + smectite 3%, quartz 10%, calcite 20%, dolomite 2%, and gypsum 20% (Cantón *et al.*, 2001). The climate is characterized by a particularly strong water deficit during the summer months. The average annual temperature is 17.9°C, with an absolute maximum of 45°C and absolute minimum of −4.5°C, and average annual rainfall is 235 mm (estimated from a 30-year record of the Tabernas weather station), with high inter- and intra-annual variability. The maximum, 24 h rainfall during the study period was 76 mm. Rainfall intensity in the region exceeds 100 mm h^{-1} only for a 5 min interval, or 150 mm h^{-1} for intervals under 1 min. Annual potential evapotranspiration is around 1500 mm, which indicates a considerable annual water deficit.

2.2. Specimens

We sampled four biological soil crust (BSC) types that are very common and abundant in the Tabernas Desert. One of them is dominated by cyanobacteria and the others by chlorolichens classified as three different lichen crust types: *Lepraria crassissima, Diploschistes diacapsis,* and *Squamarina lentigera*. The crust types were selected based on the work of Lázaro *et al.* (2008), who classified BSC types in the Tabernas Desert according to their development stage, using crust composition and color as indicators. The main characteristics of these BSCs are as follows:

(1) BSC dominated by cyanobacteria (Fig. 1). The crust is made up of diverse species, with a relatively high proportion of *Microcoleus* sheath material. This crust seems to be a primary colonizer of bare soils and progressively, when the environmental conditions are suitable, is replaced by more evolved BSCs dominated mainly by lichens (Lázaro *et al.*, 2008; Louise-Bevan, 2008).

(2) BSC dominated by *L. crassissima* (Fig. 1). This highly diverse crust is associated with small lichen species (*Collema* spp., *Placynthium nigrum*, and *Toninia sedifolia*) and cyanobacteria, and is typically found on steep north-facing slopes, where it is only able to colonize the shadiest spaces among vascular plants (Lázaro *et al.*, 2008; Louise-Bevan, 2008).

(3) BSC dominated by *D. diacapsis* (Fig. 1). This crust forms large plate-like mats. It is scattered around a variety of microhabitats and covers mostly gentle slopes with any orientation, including completely exposed, flat areas, and pediments (Lázaro *et al.*, 2008; Louise-Bevan, 2008).

(4) BSC dominated by *S. lentigera* (Fig. 1). This squamulose lichen-crust colonizes predominantly intensely rugged microhabitats on slopes, with a preference for the eastern orientation. It is particularly fragile when dry due to its rough morphology (Lázaro *et al.*, 2008; Louise-Bevan, 2008).

2.3. Raman spectroscopy

Micro-Raman spectra were collected with a miniaturized handheld instrument, the Deltanu Inspector Raman spectrometer, with a Nuscope microscope attachment and 100× magnification lens. Laser excitation was at 785 nm. The spot size was 35 μm. Lichens were placed on a manual

mobile platine with no optical fiber. The highest laser power available was 120 mW at the source. However, of the power settings available (*i.e.*, very low, low, medium, high, and very high), we chose between the very low and the low intensities to avoid damage to the sample by heating.

To improve the signal-to-noise ratio, we used 1–5 s exposure time and 5–10 accumulations. The spectral resolution was 8, 10, and 12 cm^{-1}, but for compound identification we usually used 8 cm^{-1}. The wavenumber range was 200–2000 cm^{-1}.

Our Raman analyses in a laboratory located at the University of Burgos (Spain) were first performed on dry specimens collected after a long period of drought. Samples were then sprayed with water and, after approximately 10 min, analyzed again. After finding that results could only be acquired from humid samples, field analyses were repeated during three rainy days. The Raman spectra were performed under shelter to protect both spectrometer and computer from water. Nevertheless, experimental parameters, such as temperature, humidity, wind, and altitude did not change from the original field sampling area.

A large number of areas (an average of 30 different spots) were surveyed on each specimen for a more complete knowledge of the biopigments. This procedure also provides a rough idea of the prevalence of biomolecules, since the most abundant pigment will appear in more spectra than scarcer ones.

2.4. Topographical attributes

The locations of the different BSC types (*D. diacapsis, S. lentigera, L. crassissima*, and cyanobacteria) were recorded at 96 points during the sampling campaigns with a Differential Geo Positioning System. The most important topographical attributes of each point were derived from a 1 m resolution digital elevation model (DEM) with the Idrisi GIS (version Kilimanjaro) and the Solar Analyst 1.0 extension of the ArcGis (version 8.1) GIS software. The terrain attributes extracted were

(i) Altitude;
(ii) Slope gradient;
(iii) Gradient on orientations from least to most exposed to insolation, according to the orientation classes established by Parker (1982) for calculating the Topographic Relative Moisture Index (TRMI);
(iv) Contributing area (ARE), which is the specific area that drains into each site, with use of a single-drainage-direction algorithm (Quinn *et al.*, 1991);
(v) Wetness index (W), developed by Beven and Kirkby (1979), related to the spatial distribution and size of zones of saturation or variable source areas for runoff generation. Moore *et al.* (1988) found a strong correlation between the distribution of W and the distribution of surface soil water content.

$$W = \mathrm{In.}\left(\frac{\mathrm{ARE}}{\tan.\ \mathrm{Slope}}\right)$$

(vi) Slope length factor (LSF), which is an index for the potential sediment transport with use of an algorithm derived from the unit stream power theory (Moore and Burch, 1986)

$$\mathrm{LSF} = \left[\left(\frac{\mathrm{ARE}}{22.13}\right)\cdot n \cdot \left(\sin\frac{\mathrm{Slope}}{0.0896}\right)\cdot m\right]$$

where n and m are constants ($n = 0.4$, $m = 1.3$).

(vii) Global, direct, and diffuse solar radiation at summer and winter solstices and at equinoxes. Direct solar radiation analysis was carried out with a simple transmission model for each location (List, 1971; Gates, 1980; Pearcy *et al.*, 1989; Rich, 1989, 1990), and the direct radiation received was calculated based on the position of the Sun, atmospheric attenuation, and surface orientation. For diffuse solar radiation, the standard model, which considers that the diffuse radiation varies with zenith angle, was used (Pearcy *et al.*, 1989; Rich, 1989, 1990). Global radiation for each location was found as the sum of the direct and diffuse radiation.
(viii) Hours of insolation received by each sampling point at summer and winter solstices and equinoxes.

For each sampling point, terrain and radiation attributes were calculated from the averages of nine values found from 3×3 m windows (3×3 pixels).

3. Results

3.1. Raman spectroscopy results

3.1.1. Cyanobacteria. There is no evidence of scytonemin, chlorophyll, or carotenoids in any of the Raman spectra collected on cyanobacteria with our portable Deltanu Inspector Raman spectrometer. The absence of these molecules in the spectra could be related to the characteristics of the mini-Raman instrument. It is also possible that it results from low cell densities in the crust or from a masking of the signal by the mucilaginous sheath material. Signatures at 1416, 1408, 1359, and 945 cm^{-1} suggest a mycosporine-like amino acid (MAA), whereas the 1596, 1540, 1539, 1237, 1187, 1038, 894, 746, 684, 598, 553, and 381 cm^{-1} bands could be assigned to amino acids, such as L-phenylalanine, L-tyrosine, and L-triptophane (Fig. 2).

3.1.2. Lichens. In the analysis of dried lichens, spectra show strong fluorescence, and no Raman signatures appear in any of the spectra acquired. However, Raman spectra of moist lichens show broad bands (Table 1). Biomolecules usually display complex Raman spectra, with numerous signatures, particularly in the wavenumber range 1600–900 cm^{-1}. Because of the size of the spot analyzed (35 μm) while using our handheld Raman spectrometer, signatures of more than one pigment may contribute to the same Raman feature; this is reflected as a broad band in the spectra. The low spectral resolution also contributes to this phenomenon. As a result, the new signature would neither be centered at any position of the characteristic molecular signatures of any compound nor at the average place for the specific wavenumber of each compound. Instead, it would have shifted unknown wavenumbers to higher or lower regions of the Raman spectrum, making correct biomolecular assignment very difficult.

3.1.2.A. Squamarina lentigera. The Raman bands at 1492, 1388, 1325, 1074, 980, and 914 cm^{-1} were assigned to

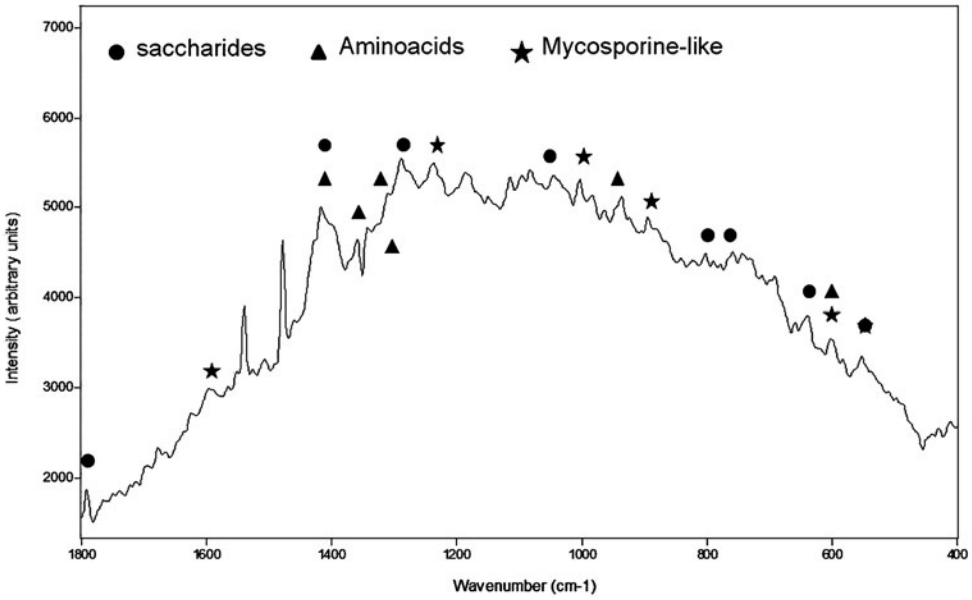

FIG. 2. Raman spectrum achieved on cyanobacteria colony showing bands assigned to mycosporine-like amino acids, saccharides, and amino acids.

chlorophyll, whereas signatures at 1521, 1153 cm^{-1} are characteristic of a carotenoid. Both bands are related to the stretching vibration of the C═C and C–C carotenoid backbone chains, respectively, and suggest the presence of zeaxanthine. Parietin could also be identified because of the bands at 1587, 1540, 1466, 1388, 1286, 1190, 980, 842, 620, 582, 431, 383, and 323 cm^{-1}; signatures at 1760, 1587, 521, 1487, 1466, 1340, 1286, 1250, 1190, 997, 701, 646, 620, 504, and 431 cm^{-1} could indicate that rhizocarpic acid was also produced by this lichen, and bands at 1629, 1604, 1530, 1480, 1462, 1323, 1287, 1184, 1152, 1142, 1070, and 992 cm^{-1} could be related to usnic acid. Calcium oxalate monohydrate (whewellite) was identified by the Raman signatures at 1488, 1466, and 504 cm^{-1}.

3.1.2.B. Diploschistes diacapsis. A weak signature centered at 1503 cm^{-1} could be associated with decaprene-beta-carotene, a long-chain carotenoid, and the band at 1505 cm^{-1} to astaxanthine, whereas the peak at 1520 cm^{-1} could be related to zeaxanthine. The broad signature at 1322 cm^{-1} was related to chlorophyll.

Bands at 1689, 1594, 1460, 1351, 1284, 1184, 1127, 985, 692, 601, and 537 cm^{-1} and signatures at 1786, 1735, 1680, 1594, 1503, 1351, 1284, 1184, 1033, 979, 780, 711, 780, 692, and 601 cm^{-1} could be assigned to usnic acid and rhizocarpic acid, respectively. We could infer the presence of emodin from 1700, 1665, 1589, 1416, 1290, 1136, 1096, 939, 495, and 468 cm^{-1} peaks, although some of its characteristic signatures do not appear in the spectrum. Strong broad bands centered at 1290 and 1416 cm^{-1} along with 1096 cm^{-1} could be related with a saturated fatty acid, but this assignment is doubtful.

3.1.2.C. Lepraria crassissima. Raman bands at 1753, 1713, 1676, 1380, 1315, 1287, 1135, 1082, and 1029 cm^{-1} could be related to the presence of fumarprotocetraric acid, and the

Table 1. Results for Different Lichens and Cyanobacteria under Different Experimental Conditions

	Cyanobacteria	*Squamarina lentigera*	*Diploschistes diacapsis*	*Lepraria crassissima*
Deltanu Inspector Raman Dry samples	- No results	- No results	- No results	- No results
Deltanu Inspector Raman Wet samples	- Maltose/glucose - L-phenylalanine	- Chlorophyll - Zeaxantine/ lutein (CAR)	- Chlorophyll - Axtaxanthine (CAR)	- Chlorophyll - Zeaxantine/lutein (CAR)
	- L-tyrosine	- Parietin	- Decapreno/ beta-carotene (CAR)	- Fumarprotocetraric acid
	- L-triptophane	- Rhizocarpic acid	- Emodin	- Calycin
	- Mycosporine-like amino acid (MAA)	- Usnic acid	- Rhizocarpic acid	- Weddellite (OX)
		- Whewellite (OX)	- Usnic acid - Whewellite (OX)	- Whewellite (OX) - Unknown compound

CAR, carotenoid; OX, oxalate.

signatures at 1604, 1592, 1483, 1378, 1348, 1315, 1242, 1111, 1029, 1002, and 943 cm^{-1} could be assigned to calycin. Lutein, a carotenoid, could be identified because of the 1525 and 1154 cm^{-1} bands. Some Raman spectra show signatures of calcium oxalate dihydrate (weddellite) at 1473 and 910 cm^{-1} with shoulders of calcium oxalate monohydrate (whewellite), centered at 1468 and 1486 cm^{-1}. A very weak broad feature centered at 1320 cm^{-1} was related to chlorophyll.

3.2. Topographical attributes

Although there is little difference in the altitude and slope range of the biological crust types analyzed (*Diploschistes diacapsis, Squamarina lentigera, Lepraria crassissima*, and cyanobacteria) (Table 2), there are differences between *L. crassissima* and the other lichen species (*D. diacapsis* and *S. lentigera*), and cyanobacteria as well, in the results for the *W* and LSF topographical indices and for the ARE (Table 2). In general, the *L. crassissima* ARE, LSF, and *W* indices were higher than *D. diacapsis, S. lentigera,* and cyanobacteria (Table 2). *L. crassissima*, *D. diacapsis, S. lentigera,* and cyanobacteria were also observed to differ in the TRMI. Eighty percent of *L. crassissima* sampled was facing north, while 56.6% of *D. diacapsis* and *S. lentigera* lichens sampled faced preferentially east and west and 10.7% south. Forty percent of the cyanobacteria faced east-west and 23.3% south.

Some differences were also observed in the direct, diffuse, and global incident solar radiation during both the equinoxes and solstices among *L. crassissima*, *D. diacapsis*, *S. lentigera,* and cyanobacteria. *L. crassissima* had lower global, direct, and diffuse incident solar radiation at the equinoxes and solstices than the other lichens and cyanobacteria (Table 2). However, it is noteworthy that, in the winter solstice, diffuse incident solar radiation was even higher than direct solar radiation (diffuse = 402 W m^{-2}) for this lichen. Cyanobacteria showed slightly higher incident solar radiation (diffuse, direct, and global) at the winter solstice and equinoxes, and lower at the summer solstice (Table 2), than *D. diacapsis* and *S. lentigera*. The number of hours of incident sunlight is very similar for all species, although somewhat lower for *L. crassissima* (Table 2).

4. Discussion

4.1. Raman spectroscopy of pigments and biomolecules in extremophile organisms and their ecophysiological functions

The fact that analysis of dry lichens generated no recognizable Raman signatures in the spectra and analysis of wet specimens generated bands that are clearly distinguishable from fluorescence (Table 1) is strikingly different from analyses performed in a laboratory of the University of Bradford (UK) on other lichen species (Edwards *et al.*, 2003a, 2003b, 2003c, 2005; Jorge-Villar *et al.*, 2005a; Jorge-Villar and Edwards, 2010). In those analyses, there was no problem in acquiring and identifying biopigments from the Raman spectra. This could be explained, on the one hand, by the characteristics of the handheld spectrometers, which may have technical limitations that restrict their capacity to detect weak signals. On the other hand, the lack of recognizable Raman signatures could be due to the physical status of desiccated cells and molecules of terriculous lichens living in the extreme environment of the Tabernas Desert. Heber *et al.* (2007, 2010) documented a reversible inactivation of photosystem II upon desiccation in cyanolichens, presumably as a photoprotective mechanism. They concluded that the desiccation induced conformational changes of the pigment–protein complex, which resulted in the fast radiationless dissipation of absorbed light energy. Energy dissipation is inactivated and structural changes are reversed when water

Table 2. Topographical Attributes at the Sampling Locations of Each Biological Soil Crust Type

	Cyanobacteria	Lichens *D. diacapsis* and *S. lentigera*	Lichen *L. crassissima*
	Av ± *SD*	*Av* ± *SD*	*Av* ± *SD*
Altitude (m)	266 ± 11	271 ± 17	265 ± 21
TRMI (Topographic Relative Moisture Index)	36.7% North, 40% East-West, 23.3% South	35.7% North, 53.6% East-West, 10.7% South	80% North, 20% East-West
Slope (%)	26 ± 13	23 ± 11	28 ± 10
W (Wetness index)	4 ± 2	4 ± 1	5 ± 2
ARE (Contributing area) (m^2 m^{-1})	35 ± 62	36 ± 68	264 ± 446
LSF (Slope length factor)	10 ± 8	9 ± 7	24 ± 21
Global solar radiation at summer solstice (W m^{-2})	6538 ± 711	6779 ± 620	6345 ± 684
Direct solar radiation at summer solstice (W m^{-2})	5128 ± 598	5317 ± 518	4942 ± 576
Diffuse solar radiation at summer solstice (W m^{-2})	1410 ± 172	1462 ± 154	1403 ± 159
Hours of insolation at summer solstice (h)	12 ± 2	12 ± 1	12 ± 2
Global solar radiation at winter solstice (W m^{-2})	1341 ± 745	1160 ± 557	596 ± 249
Direct solar radiation at winter solstice (W m^{-2})	844 ± 760	644 ± 554	101 ± 216
Diffuse solar radiation at winter solstice (W m^{-2})	497 ± 61	515 ± 55	495 ± 57
Hours of insolation at winter solstice (h)	5 ± 3	4 ± 3	1 ± 2
Global solar radiation at equinox (W m^{-2})	3938 ± 1073	3890 ± 876	3076 ± 682
Direct solar radiation at equinox (W m^{-2})	2915 ± 1080	2829 ± 859	2058 ± 626
Diffuse solar radiation at equinox (W m^{-2})	1023 ± 125	1061 ± 112	1018 ± 116
Hours of insolation at equinox (h)	9 ± 1	9 ± 1	8 ± 2

Av ± SD, average ± standard deviation.

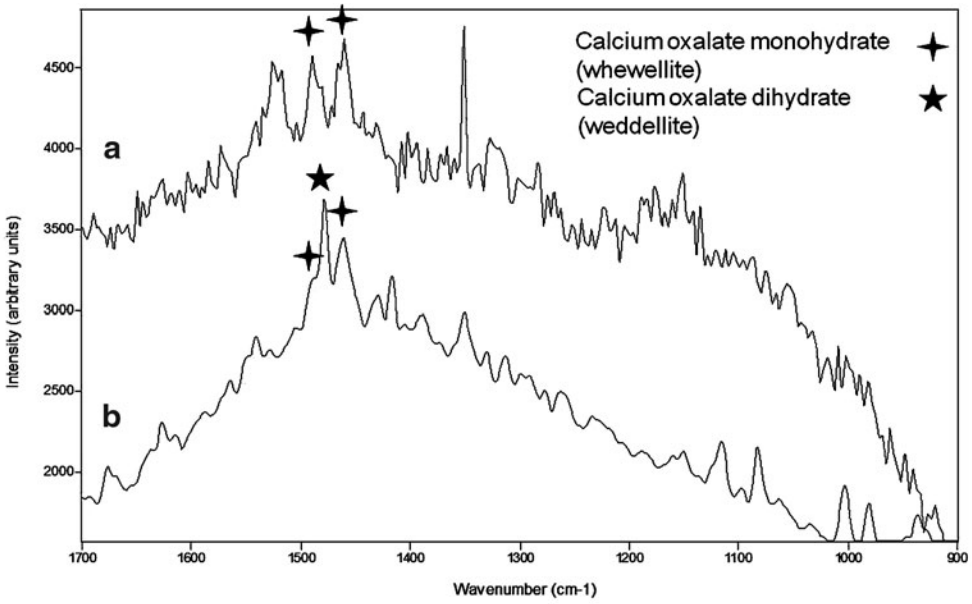

FIG. 3. Raman bands identifying calcium oxalates whewellite and weddellite in *Squamarina lentigera* (Spectrum a) and *Lepraria crassissima* (Spectrum b).

becomes available again (Heber, 2008). The increase in the reflectivity of dry versus wet specimens could interact with the instrument and contribute to decrease its sensitivity even more.

Raman spectra of cyanobacteria in the Tabernas Desert do not show evidence of scytonemin, chlorophyll, or carotenoids, although those pigments were detected in cyanobacteria specimens from other areas analyzed by our group in other projects (Chu *et al.*, 1998; Edwards *et al.*, 1999, 2004c, 2005; Wynn-Williams *et al.*, 2000; Jorge-Villar *et al.*, 2005b, 2006). Nevertheless, these organisms did show evidence of compounds such as saccharides (maltose, glucose, or both), amino acids (L-phenylalanine, L-tyrosine, and L-triptophane), and MAA (Fig. 2). The exopolysaccharides excreted could be carrying out an important protective role against desiccation and UV irradiation in the cyanobacteria (Knowles and Castenholz, 2008; Chen *et al.*, 2009).

Regarding the protective pigments in the lichen samples found by Raman spectroscopy, the spectra show that chlorophyll, a photosynthetic pigment, was present in all lichens. The miniaturized Raman spectrometer was unable to discern different types of chlorophyll from the spectra; however, we can propose assignment of carotenoid types (Table 1). In *S. lentigera* and *L. crassissima,* carotenoids were assigned to zeaxanthine or lutein, respectively, whereas in *D. diacapsis* astaxanthine, zeaxanthine, and decapreno-beta-carotene were identified. The dual role of carotenoids as efficient UV photoprotective molecules (Cockell and Knowland, 1999) and auxiliary DNA repair agents (Edwards *et al.*, 2006; Edwards, 2007) has been recognized in extremophile colonies. Carotenoid pigments also quench the excess energy not used photosynthetically (especially UVB), which would otherwise generate highly toxic singlet oxygen (Cockell and Knowland, 1999).

Based on the large number of Raman spectra acquired for each lichen specimen, we can suggest that there are differences, not only in the type of oxalate produced by these organisms but also in the relative proportion in which those biomolecules appear (Fig. 3). *L. crassissima* showed mono- and dihydrate calcium oxalates (whewellite and weddellite, respectively), from which weddellite was significantly more abundant. In *S. lentigera,* calcium oxalate monohydrate (whewellite) was observed, and no bands of weddellite appeared. Only one spectrum on *D. diacapsis* shows signatures of calcium oxalates, in this case whewellite. The ability of lichens to exude calcium oxalates is associated with a significant antidesiccative water-storage strategy for their survival in extremely dry habitats (Edwards *et al.*, 1997, 2003d; Seaward and Edwards, 1997; Holder *et al.*, 2000; Jorge-Villar *et al.*, 2004, 2005a, 2006; Jorge-Villar and Edwards, 2010) and also as a strategy for removing oxalic acid as waste from the Krebs metabolic cycle (Edwards *et al.*, 1997; Seaward and Edwards, 1997; Jorge-Villar *et al.*, 2005a, 2005b; Edwards, 2007).

Other pigments with an important protective role against photostress and oxidation were also found in the lichen communities analyzed in this work (Table 1). Specifically, rhizocarpic acid (antioxidant pigment that acts as a free energy quenching molecule; Wynn-Williams and Edwards, 2000; Jorge-Villar *et al.*, 2006) and usnic acid (UV-radiation screening pigment; Jorge-Villar *et al.*, 2006) could be present in both *S. lentigera* and *D. diacapsis*. *S. lentigera* may also yield parietin, whereas *D. diacapsis* could produce emodin, both compounds acting as UV-radiation screening.

Lepraria crassissima seems to show the most varied protective strategies, not only with regard to the quantity and variety of oxalates but also in the type of biopigments, since calycin and fumarprotocetraric acid (UV-radiation screening pigments) were identified by Raman spectroscopy.

4.2. Relationships between topographic attributes and protective pigment in extremophile organisms

The topographic attributes extracted from the DEM show that lichens and cyanobacteria communities were not randomly distributed but seem to have been associated with

some topographic features and microclimates, which is in agreement with findings of other authors (Sancho and Valladares, 1993; Green *et al.*, 1994; Palmqvist and Sundberg, 2000; Gaio-Oliveira *et al.*, 2004; Lázaro *et al.*, 2008). At the same time, the results obtained with the handheld Deltanu Inspector Raman spectrometer suggest that such communities could have adopted different stress-avoidance strategies by producing biological metabolites that would have allowed them to adapt successfully to these microclimates and dominate within specific microniches. The differences among pigments and biomolecules found by Raman spectroscopy in the organisms studied could be related to different metabolic responses to some parameters, such as incident radiation and humidity, as well as their varied ability to achieve hydration.

The cyanobacteria were predominantly located in areas with the highest global and direct radiation levels (Table 2). Their Raman spectra show evidence of effective UV-screening compounds, such as MAAs with maximal UV absorption in the 310–360 nm range (Edwards *et al.*, 2005). Increased MAA concentrations associated with increases in UV flux have been observed in organisms directly in the field (Cockell and Knowland, 1999). This type of screening compound over other response data demonstrates the importance of elucidating the complete range of UV responses in a given organism. Therefore, although wide surveys of UV screening compounds in nature can be of initial value, interpretation of the data in the ecological context must be undertaken with great care. On the other hand, MAAs may have other physiological functions as well as UV screening; for example, cyanobacteria in some high-salt environments, where MAAs with an internal cell concentration of 98 mmol L^{-1} have been found to be produced in response to increasing salt concentrations. In this case, they are presumed to have a role in balancing the osmotic pressure inside the cells to counteract water loss (Oren, 1997).

Diploschistes diacapsis and *S. lentigera* lichens can also exist in a variety of microhabitats and are able to colonize sites with comparatively high solar radiation (Table 2). In contrast, *L. crassissima* is found mainly on north-facing slopes, where solar radiation is at its lowest (Table 2). Despite these differences, all lichen species analyzed developed pigments with a photoprotective role. Nevertheless, it is worth mentioning that *D. diacapsis* and *S. lentigera* produced the highest number of pigments with UVB (*e.g.*, usnic acid, emodin, parietin, beta-carotene) as well as with UVC radiation protection (*e.g.*, beta-carotene, rhizocarpic acid, usnic acid, parietin), the latter the most energetic and most harmful radiation. This could suggest that, although individually these pigments could not protect the lichens from the complete range of UV radiation, together they may act as an effective UV radiation screen, since the range that each one covers overlaps with that of the others. Since the microhabitats colonized by the specific lichens are more exposed to direct solar radiation, it is possible that this mechanism has been adopted as a survival strategy. This way they have succeeded in developing a comparatively better adaptive capacity over other lichen species, such as *L. crassissima*. Nevertheless, it is interesting to note that although *L. crassissima* is still only able to colonize those areas with little solar radiation, it also showed UV-radiation screening pigments, which could be explained by the relatively high rates of diffuse radiation achieved in areas usually colonized by this community (Table 2).

The different lichen specimens studied here seem to colonize microniches with different water availability (different contributing areas and wetness; Table 2), which suggests that they could have different moisture requirements and different hydration strategies. In this regard, notice that Raman spectra of *L. crassissima*, which colonize habitats with the largest water-contributing areas and lowest insolation rates (Table 2), showed the highest concentration of mono- and especially dihydrate calcium oxalate (Table 1, Fig. 3). Previous studies of lichen colonization in different environments have shown that the presence of sufficient available moisture encourages the formation of dihydrate calcium oxalate (Holder *et al.*, 2000; Edwards, 2007). Therefore, the preferential formation of weddellite in *L. crassissima* may be related with the higher availability of moisture in the microhabitats usually occupied by this species. The use of weddellite by *L. crassissima* communities in the Tabernas Desert could be associated with water storage strategies and tolerance in this desiccated habitat, as also reported by other authors (Edwards *et al.*, 1997, 2003d; Seaward and Edwards, 1997; Holder *et al.*, 2000; Jorge-Villar *et al.*, 2004, 2005a, 2006; Jorge-Villar and Edwards, 2010). In contrast, *D. diacapsis* and *S. Lentigera,* which cover locations that receive higher global and direct solar radiation and lower moisture indices than for *L. crassissima,* showed comparatively lower concentrations of calcium oxalate monohydrate in their Raman spectra (Table 2) and could not, therefore, be contributing to the formation of calcium oxalate dihydrate. In this case, both lichens may have developed other hydration mechanisms.

5. Conclusions

We have undertaken a study of the distribution of three extremophile lichens and a bacterial community in the Tabernas Desert, southeastern Spain, and analyzed topography-related environmental factors of their habitats, such as direct and diffuse incident solar radiation and water availability. We employed a handheld Raman spectrometer to identify oxalates and protective pigments produced by those organisms, and GIS methods to extract the DEM-related parameters.

The evidence from this study suggests that the specific field distribution of lichens and cyanobacteria is related to the topography. Each community is adapted to specific environmental conditions of insolation and wetness, as reflected in their adaptive strategies, such as the protective pigment production or the presence of calcium oxalates. Raman spectroscopy data show that *D. diacapsis* and *S. lentigera* lichen communities, which are exposed to the highest rates of incident solar radiation, produce a high number of protective pigments that could play complementary roles. However, *L. crassissima*, which colonizes areas with lower insolation rates, generates fewer protective pigments. The cyanobacterial community has developed very different strategies from those of the lichens, which could be related to the severe environmental parameters, since they are the first colonizers on soils and withstand the most hazardous conditions.

Our data also reflect agreement between humidity parameters and the presence of calcium oxalate monohydrate and/or calcium oxalate dihydrate. Where humidity was

higher, lichens produced both oxalates, whereas with less humidity only calcium oxalate monohydrate was produced. Although it looks like lichens had enough water for survival under the wettest conditions, *L. crassissima* might require extra water storage and, therefore, produces weddellite to supply it.

Surprisingly, there were no clear Raman signals when the analyses were performed with our portable Raman spectrometer on the four extremophile organisms sampled during a long drought. It is obvious that this lack of results cannot be interpreted as absence of life. There could be several reasons for this phenomenon. First, the design and construction of the miniaturized instrument could have a negative impact on the resolution of the spectrometer and therefore on its capacity to obtain useful results. The increase in reflectivity of dry versus wet specimens could reduce the sensitivity of the instrument even further. It is also possible that reversible changes in the chemical makeup of the organisms under desiccation, for example, desiccation-induced conformational changes in a pigment-protein complex, could be responsible for the lack of signals. This issue is of particular relevance to extraplanetary exploration, where miniaturized analytical instruments could be utilized for the study of extremophile organisms living under severe conditions. A better understanding of Raman spectrometer limitations is, therefore, a prerequisite for employing such instruments in extraplanetary missions. Although this is already being taken into account, our results stress the need for employing a sample manipulation protocol so that the selected specimens are analyzed under optimal environmental conditions as well as handling parameters, namely, humidity, temperature, or light.

Acknowledgments

The authors wish to thank the GEOCARBO (Ref. RNM-3721) and the COSTRAS (Ref. RNM-3614) projects funded by the regional government of Andalucía (Spain); the BACARCOS project (Ref. CGL2011-29429) and CARBORAD (CGL2011-27493) projects funded by the Spanish Ministry of Science and Innovation, the European Regional Development Fund (ERDF), and the Juan de la Cierva Fellowship (Ref. 2008-39669).

Abbreviations

ARE, contributing area; BSC, biological soil crust; DEM, digital elevation model; GIS, Geographic Information System; LSF, slope length factor; MAA, mycosporine-like amino acid; TRMI, Topographic Relative Moisture Index; *W*, wetness index.

References

Beven, K.J. and Kirkby, M.J. (1979) A physically based, variable contribution area model of basin hydrology. *Hydrological Sciences Bulletin* 24:43–69.

Bryan, R.B. and Yair, A. (1982) Perspectives on studies of badland geomorphology. In *Badlands Geomorphology and Piping*, edited by R. Bryan and A. Yair, Geo Books, Norwich, UK, pp 1–12.

Campbell, I.A. (1989) Badlands and badlands gullies. In *Arid Zone Geomorphology*, edited by D.S.G. Thomas, Halstead Press, New York, pp 159–183.

Cantón, Y., Solé-Benet, A., Queralt, I., and Pini, R. (2001) Weathering of a gypsum-calcareous mudstone under semiarid environment at Tabernas, SE Spain: laboratory and field-based experimental approaches. *Catena* 44:111–132.

Chen, L.Z., Wang, G.H., Hong, S., Liu, A., Li, C., and Liu, Y.D. (2009) UV-B-induced oxidative damage and protective role of exopolysaccharides in desert cyanobacterium *Microcoleus vaginatus*. *J Integr Plant Biol* 51:194–200.

Chu, F.J., Seaward, M.R.D., and Edwards, H.G.M. (1998) Application of FT-Raman spectroscopy to an ecological study of the lichen *Xanthoparmelia scabrosa* in the supralittoral zone, Hong Kong. *Spectrochim Acta A* 54:967–982.

Cockell, C.S. and Knowland, J. (1999) Ultraviolet radiation screening compounds. *Biol Rev Camb Philos Soc* 74:311–345.

Dickensheets, D.L., Wynn-Williams, D.D., Edwards, H.G.M., Crowder, C., and Newton, E.M. (2000) A novel miniature confocal microscope/Raman spectrometer system for biomolecular analysis on future Mars missions after Antarctic trials. *J Raman Spectrosc* 31:633–635.

Dillon, J.G., Tatsumi, C.M., Tandingan, P.G., and Castenholz, R.W. (2002) Effect of environmental factors on the synthesis of scytonemin, a UV-screening pigment, in a cyanobacterium (*Chroococcidiopsis* sp.). *Arch Microbiol* 177:322–331.

Edwards, H.G.M. (2007) A novel extremophile strategy studied by Raman spectroscopy. *Spectrochim Acta A* 68:1126–1132.

Edwards, H.G.M., Russell, N.C., and Wynn-Williams, D.D. (1997) Fourier transform Raman spectroscopic and scanning electron microscopic study of cryptoendolithic lichens from Antarctica. *J Raman Spectrosc* 28:685–690.

Edwards, H.G.M., Farwell, D.W., Grady, M.M., Wynn-Williams, D.D., and Wright, I.P. (1999) Comparative Raman spectroscopy of a martian meteorite and Antarctic lithic analogues. *Planet Space Sci* 47:353–362.

Edwards, H.G.M., Newton, E.M., Dickensheets, D.L., and Wynn-Williams, D.D. (2003a) Raman spectroscopic detection of biomolecular markers from Antarctic materials: evaluation for putative martian habitats. *Spectrochim Acta A* 59:2277–2290.

Edwards, H.G.M., Newton, E.M., Wynn-Williams, D.D., and Coombes, S.R. (2003b) Molecular spectroscopic studies of lichen substances. I. Parietin and emodin. *J Mol Struct* 648: 49–59.

Edwards, H.G.M., Newton, E.M., and Wynn-Williams, D.D. (2003c) Molecular structural studies of lichen substances. II. Atranorin, gyrophoric acid, fumarprotocetraric acid, rhizocarpic acid, calycin, pulvinic dilactone and usnic acid. *J Mol Struct* 651:27–37.

Edwards, H.G.M., Seaward, M.R.D., Attwood, S.J., Little, S.J., Oliveira, L.F.C., and Tretiach, M. (2003d) FT-Raman spectroscopy of lichens on dolomitic rocks: an assessment of metal oxalate formation. *Analyst* 128:1218–1221.

Edwards, H.G.M., Wynn-Williams, D.D., Little, S.J., Oliveira, L.F.C., Cockell, C.S., and Ellis-Evans, J.C. (2004a) Stratified response to environmental stress in a polar lichen characterized with FT-Raman microscopic analysis. *Spectrochim Acta A* 60:2029–2033.

Edwards, H.G.M., Wynn-Williams, D.D., and Jorge-Villar, S.E. (2004b) Biological modification of haematite in Antarctic cryptoendolithic communities. *J Raman Spectrosc* 35:470–474.

Edwards, H.G.M., Jorge-Villar, S.E., Moody, C.D., and Mancinelli, R. (2004c) Raman spectroscopy of desert varnishes and their rock substrata. *J Raman Spectrosc* 35:475–479.

Edwards, H.G.M., Moody, C.D., Jorge-Villar, S.E., and Wynn-Williams, D.D. (2005) Raman spectroscopic detection of key

biomarkers of cyanobacteria and lichen symbiosis in extreme Antarctic habitats: evaluation for Mars lander missions. *Icarus* 174:560–571.

Edwards, H.G.M., Moeller, R., Jorge-Villar, S.E., Horneck, G., and Stackebrandt, E. (2006) Raman spectroscopic study of the photoprotection of extremophilic microbes against ultraviolet radiation. *International Journal of Astrobiology* 5:313–318.

Ehling-Schulz, M., Bilger, W., and Scherer, S. (1997) UV-B-induced synthesis of photoprotective pigments and extracellular polysaccharides in the terrestrial cyanobacterium *Nostoc commune*. *J Bacteriol* 179:1940–1945.

Gaio-Oliveira, G., Dahlman, L., Máguas, C., and Palmqvist, K. (2004) Growth in relation to microclimatic conditions and physiological characteristics of four *Lobaria pulmonaria* populations in two contrasting habitats. *Ecography* 27:13–28.

Garcia-Pichel, F. and Castenholz, R.W. (1991) Characterization and biological implications of scytonemin, a cyanobacterial sheath pigment. *J Phycol* 27:395–409.

Gates, D.M. (1980) *Biophisycal Ecology,* Springer-Verlag, New York.

Green, T.G.A., Lange, O.L., and Cowan, I.R. (1994) Ecophysiology of lichen photosynthesis: the role of water status and thallus diffusion resistances. *Cryptogamic Botany* 4:166–178.

Heber, U. (2008) Photoprotection of green plants: a mechanism of ultra-fast thermal energy dissipation in desiccated lichens. *Planta* 228:641–650.

Heber, U., Azarkovich, M., and Shuvalov, V. (2007) Activation of mechanisms of photoprotection by desiccation and by light: poikilohydric photoautotrophs. *J Exp Bot* 58:2745–2759.

Heber, U., Bilger, W., Türk, R., and Lange, O.L. (2010) Photoprotection of reaction centres in photosynthetic organisms: mechanisms of thermal energy dissipation in desiccated thalli of the lichen *Lobaria pulmonaria*. *New Phytol* 185:459–470.

Holder, J.M., Wynn-Williams, D.D., Rull-Perez, F., and Edwards, H.G.M. (2000) Raman spectroscopy of pigments and oxalates *in situ* within epilithic lichens: Acarospora from the Antarctic and Mediterranean. *New Phytol* 145:271–280.

Jorge-Villar, S.E. and Edwards, H.G.M. (2005) Near-infrared Raman spectra of terrestrial minerals: relevance for the remote analysis of martian spectral signatures. *Vib Spectrosc* 39:88–94.

Jorge-Villar, S.E. and Edwards, H.G.M. (2010) Lichen colonization of an active volcanic environment: a Raman spectroscopic study of extremophile biomolecular protective strategies. *J Raman Spectrosc* 41:63–67.

Jorge-Villar, S.E., Edwards, H.G.M., and Seaward, M.R.D. (2004) Lichen biodeterioration of ecclesiastical monuments in northern Spain. *Spectrochim Acta A* 60:1229–1237.

Jorge-Villar, S.E., Edwards, H.G.M., and Seaward, M.R.D. (2005a) Raman spectroscopy of hot desert, high altitude epilithic lichens. *Analyst* 130:730–737.

Jorge-Villar, S.E., Edwards, H.G.M., and Cockell, C.S. (2005b) Raman spectroscopy of endoliths from Antarctic cold desert environments. *Analyst* 130:156–162.

Jorge-Villar, S.E., Edwards, H.G.M., and Benning, L.G. (2006) Raman spectroscopic and scanning electron microscopic analysis of a novel biological colonisation of volcanic rocks. *Icarus* 184:158–169.

Knowles E.J. and Castenholz, R.W. (2008) Effect of exogenous extracellular polysaccharides on the desiccation and freezing tolerance of rock-inhabiting phototrophic microorganisms. *FEMS Microbiol Ecol* 66:261–270.

Lázaro, R., Cantón, Y., Solé-Benet, A., Bevan, J., Alexander, R., Sancho, L.G., and Puigdefábregas, J. (2008) The influence of competition between lichen colonization and erosion on the evolution of soil surfaces in the Tabernas badlands (SE Spain) and its landscape effects. *Geomorphology* 102:252–266.

List, R.J. (1971) *Smithsonian Meteorological Tables, Sixth Revised Edition*, Smithsonian Miscellaneous Collections, Vol. 114, Smithsonian Institution Press, Washington DC.

Louise-Bevan, J. (2008) Dynamics of lichen dominated biological soil crust in El Cautivo badlands, southeast Spain. Thesis. University of Liverpool, UK.

Miralles-Mellado, I., Cantón, Y., and Solé-Benet, A. (2011) Two-dimensional porosity of crusted silty soils: indicators of soil quality in semiarid rangelands? *Soil Sci Soc Am J* 75:1330–1342.

Moore, I.D. and Burch, G.J. (1986) Physical basis of the length-slope factor in the universal soil loss equation. *Soil Sci Soc Am J* 50:1294–1298.

Moore, I.D., Burch, G.J., and Mackenzie, D.H. (1988) Topographic effects on the distribution of surface soil water and the location of ephemeral gullies. *Trans ASAE* 31:1098–1107.

Nealson, K.H. (1997) The limits of life on Earth and searching for life on Mars. *J Geophys Res* 102:23675–23686.

Oren, A. (1997) Mycosporine-like amino acids as osmotic solutes in a community of halophilic cyanobacteria. *Geomicrobiol J* 14:231–240.

Palmqvist, K. and Sundberg, B. (2000) Light use efficiency of dry matter gain in five macrolichens: relative impact of microclimatic conditions and species-specific traits. *Plant Cell Environ* 23:1–14.

Parker, A.J. (1982) The topographic relative moisture index: an approach to soil moisture assessment in mountain terrain. *Physical Geography* 3:160–168.

Pearcy, R.W. (1989) Radiation and light measurements. In *Plant Physiological Ecology: Field Methods and Instrumentation*, edited by R.W. Pearcy, J. Ehleringer, H.A. Mooney, and P.W. Rundel, Chapman and Hall, New York, pp 95–116.

Quinn, P.K., Beven, K., Chevallier, P., and Planchon, O. (1991) The prediction of hillslope flow paths for distributed hydrological modelling using digital terrain models. *Hydrol Process* 5:59–79.

Rich, P.M. (1989) *A Manual for Analysis of Hemispherical Canopy Photography,* Los Alamos National Laboratory Report LA-11733-M, Los Alamos National Laboratory, Los Alamos, NM.

Rich, P.M. (1990) Characterizing plant canopies with hemispherical photography. Instrumentation for studying vegetation canopies for remote sensing in optical and thermal infrared regions. *Remote Sensing Reviews* 5:13–29.

Sancho, L.G. and Valladares, F. (1993) Lichen colonization of recent moraines on Livingston Island (South Shetland I., Antarctica). *Polar Biol* 13:227–233.

Scheidegger, A.E., Schumm, S.A., and Fairbridge, R.W. (1968) Badlands. In *The Encyclopedia of Geomorphology*, edited by R.W. Fairbridge, Reinhold Book Corporation, New York, pp 43–48.

Singh, J., Dubey, A.K., and Singh, R.P. (2011) Antarctic terrestrial ecosystem and role of pigments in enhanced UV-B radiations. *Rev Environ Sci Biotechnol* 10:63–77.

Sinha, R.P., Klisch, M., Helbling, E.W., and Hader, D.P. (2001) Induction of mycosporine-like amino acids (MAAs) in cyanobacteria by solar ultraviolet-B radiation. *J Photochem Photobiol B, Biol* 60:129–135.

Seaward, M.R.D. and Edwards, H.G.M. (1997) Biological origin of major chemical disturbances on ecclesiastical architecture studied by Fourier transform Raman spectroscopy. *J Raman Spectrosc* 28:691–696.

Wang, A., Kuebler, K.E., Jolliff, B.L., and Haskin, L.A. (2004) Raman spectroscopy of Fe-Ti-Cr-oxides, case study: martian meteorite EETA79001. *Am Mineral* 89:665–680.

Wynn-Williams, D.D. and Edwards, H.G.M. (2000) Proximal analysis of regolith habitats and protective biomolecules *in situ* by laser Raman spectroscopy: overview of terrestrial Antarctic habitats and Mars analogs. *Icarus* 144:486–503.

Wynn-Williams, D.D., Edwards, H.G.M., and Garcia-Pichel, F. (2000) Functional biomolecules of Antarctic stromatolitic and endolithic cyanobacterial communities. *Eur J Phycol* 34: 381–391.

Address correspondence to:
I. Miralles
EEZA-CSIC
04230 La Cañada de San Urbano
Almería 04120
Spain

E-mail: imirallesmellado@gmail.com

Submitted 5 November 2011
Accepted 1 May 2012